

Observation of isotropic critical spin fluctuations in Gd

Gary Scott Collins,* Aatur R. Chowdhury,† and Christoph Hohenemser
Department of Physics, Clark University, Worcester, Massachusetts 01610

(Received 12 November 1985)

Perturbed $\gamma\gamma$ angular-correlation experiments on oriented single crystals of Gd, containing 1 ppb of ^{111}In , demonstrate that critical spin fluctuations are isotropic to within about 1 K above the Curie temperature. Closer to T_C we find evidence that the critical spin fluctuations fall increasingly along the c axis. Analysis of nuclear relaxation times in the isotropic region leads to spin autocorrelation times that diverge with an exponent $w=0.53(8)$. This value is not consistent with either spin-nonconserved Heisenberg behavior or Ising behavior, but agrees with Mössbauer data for $\text{Gd } ^{161}\text{Dy}$.

Gadolinium is an S -state ion which should have predominantly isotropic exchange interactions, and, like Fe and Ni, exhibit Heisenberg critical behavior. On the other hand, Gd is noncubic, with uniaxial spin alignment along the c axis below T_C ,¹⁻³ suggesting that like MnF_2 it may exhibit Ising critical behavior. Ising critical behavior is also suggested by the observation of Ising-like domain walls near T_C .⁴

Static critical exponent measurements span both the Heisenberg- and Ising-model predictions. We have argued that nonasymptotic data may be the cause of the inconsistency in static exponent measurements.⁵ In this context we reported a new measurement of the exponent β which was more nearly asymptotic than all previous magnetic measurements.⁶ Although the result $\beta=0.399(16)$ is close to the prediction for the Heisenberg model; the presence of large corrections to scaling leaves open the possibility of eventual crossover to Ising behavior.

The question of whether Gd is described by Heisenberg or Ising critical behavior may also be addressed through a study of critical dynamics. In earlier work we have reported a Mössbauer linewidth study of critical slowing down for $\text{Gd } ^{161}\text{Dy}$, and found that the divergence of the wave-vector-averaged spin autocorrelation time could not be reconciled with either Heisenberg or Ising spin dynamics.^{5,7} A weakness of that work, however, is the fact that we had to *assume isotropy* of spin fluctuations in order to analyze the Mössbauer data.

In experiments reported here we eliminate assumptions about fluctuation isotropy that were implicit in our Mössbauer work on $\text{Gd } ^{161}\text{Dy}$. This is accomplished through nuclear relaxation studies of oriented single crystals of Gd, using the method of perturbed $\gamma\gamma$ angular correlations (PAC).

I. EXPERIMENTAL DATA

Our samples were oriented single crystals of Gd (obtained from Ames Laboratories) into which 10 μCi of carrier-free ^{111}In had been diffused. Sources were prepared by depositing ^{111}In dissolved in dilute HCl on the sample surface, evaporating to dryness, and diffusing *in vacuo* for 1 hour at 1150 K. Because of the short (2.7 d) half-life of the ^{111}In activity, its estimated concentra-

tion in the diffused sample was about 1 ppb.

The sample temperature was controlled by a two-stage thermoelectric module enclosed in a vacuum can, and temperature regulation was achieved via a thermocouple-controlled differential voltmeter. Temperature stability was better than 0.05 K.

PAC spectra were collected with a four-counter spectrometer, and reduced via methods described elsewhere.⁸ This leads to a time-dependent perturbation, $G_2(t)$, which for $T > T_C$ can be analyzed in terms of a unique axially symmetric electric quadrupole interaction.

Far above T_C nuclear relaxation is practically undetectable, and the PAC signal was fitted with the form

$$G_2(t) = 0.2 + S_1 \cos(\omega_0 t) + S_2 \cos(2\omega_0 t) + S_3 \cos(3\omega_0 t), \quad (1)$$

where $\omega_0 = (3\pi/10)e^2 Qq_{zz} = 23.5(1)$ Mrad/s is the fundamental quadrupole interaction frequency, and Q and q_{zz} are the quadrupole moment and principal component of the electric field gradient, respectively. A comparable value for ω_0 [23.4(7) Mrad/s] had been obtained in the earlier work of Boström *et al.*³ Because q_{zz} lies along the c axis, oriented single crystals give different weighting to the amplitudes in Eq. (1). For the c axis of the crystal perpendicular to the plane of the counters we found $S_1 = 0.70(2)$, $S_2 = 0.01(1)$, and $S_3 = 0.08(1)$. For the c axis of the crystal parallel to the plane of the counters and oriented at 45° with respect to a pair of neighboring counters, we found $S_1 = 0.16(2)$, $S_2 = 0.63(2)$, and $S_3 = 0.01(1)$. Figure 1 illustrates the distinctly different patterns obtained in the two orientations.

As $T \rightarrow T_C^+$ the spectra for $G_2(t)$ show increasingly strong damping which we interpret as nuclear relaxation induced by critical slowing of the electronic spin fluctuations. Examples of damped spectra for the c axis perpendicular to the plane of the counters are shown in Fig. 2. Equivalent results are obtained for the c axis parallel to the plane of the counters. [The data on which the further analysis is based were taken on two equivalent samples (named *A* and *B* in Table II and Fig. 6) with the c axis perpendicular to the plane of the detectors.]

To determine the value of T_C we used PAC data obtained in the ferromagnetic region. These were analyzed

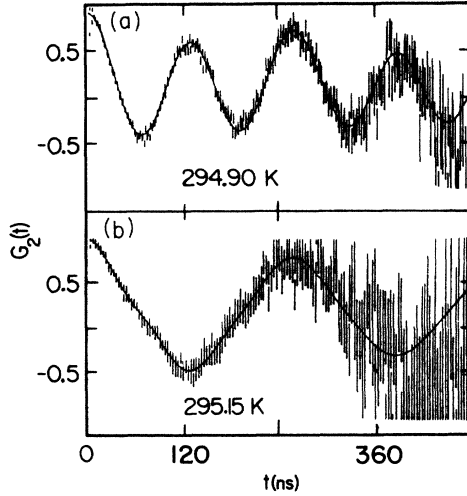


FIG. 1. Perturbed angular correlation spectra well above T_C , for the c axis in the plane and perpendicular to the plane of the counters [(a) and (b), respectively].

in terms of the hyperfine field, $H_{\text{hf}}(T)$, and as shown in detail elsewhere,⁶ may be fitted to

$$H_{\text{hf}}(T) = B(1 - T/T_C)^\beta \quad (2)$$

to extract T_C , β , and B . In this way we obtained $T_C = 291.85(5)$ K for the single-crystal sample used in the present work. Figure 3 illustrates the quality of the ferromagnetic data via a linearized plot of $H_{\text{hf}}(T)^{1/\beta}$ versus T .

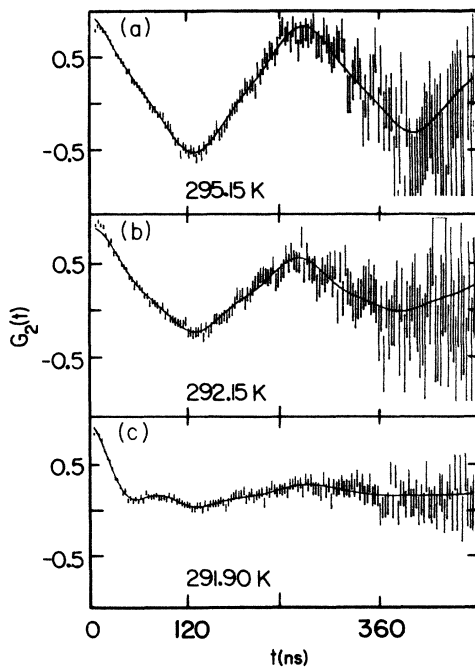


FIG. 2. Perturbed angular correlation spectra showing increasing relaxation as the temperature approaches T_C^+ [(a) to (c)].

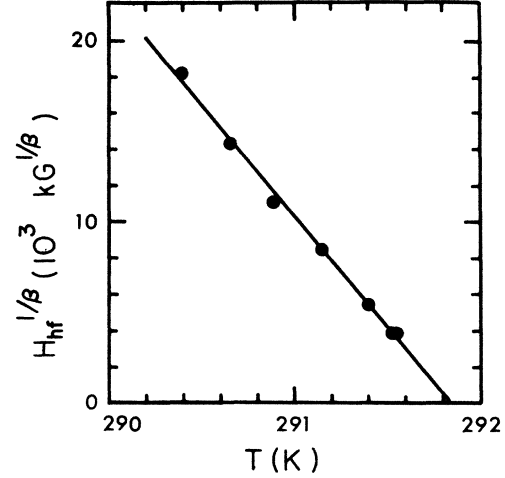


FIG. 3. Linearized plot of the hyperfine field, $H_{\text{hf}}^{1/\beta}$, below T_C used to determine that $T_C = 291.85(5)$ K. The value of the exponent β was 0.399, as determined by fitting with corrections to scaling (see Ref. 6).

II. ANALYSIS OF RELAXATION SPECTRA

To fit the spectra above T_C it is necessary to choose a relaxation model. Key to our analysis is the fact that anisotropic and isotropic spin fluctuations produce distinctly different forms for $G_2(t)$. By determining which model, isotropic or anisotropic, better fits the experimental results for $G_2(t)$ it is therefore possible to decide whether spin fluctuations are isotropic or anisotropic.

To describe isotropic electronic spin fluctuations we write

$$G_2(t) = \exp(-t/\tau_R) [S_0 + S_1 \cos(\omega_0 t) + S_2 \cos(2\omega_0 t) + S_3 \cos(3\omega_0 t)], \quad (3)$$

where the nuclear relaxation time is given by

$$\tau_R = 2S(S+1)A^2\tau_c, \quad (4)$$

and τ_c and $A = \omega_L(T=0 \text{ K})/S$ are the wave-vector-averaged spin autocorrelation time and hyperfine coupling constant, respectively. This assumes an isotropic contact interaction $\hbar \mathbf{AI} \cdot \mathbf{S}$ between the nuclear spin \mathbf{I} and the neighboring host spin, \mathbf{S} . Equations (3) and (4) are comparable to the results of Abragam and Pound⁹ and are valid in the motional narrowing limit. This requires that τ_c is the shortest time in the problem: i.e., $\tau_c \ll 2\pi/\omega_L$, $\tau_c \ll 2\pi/\omega_0$, $\tau_c \ll \tau_N$, where τ_N is the nuclear lifetime of the gamma emitting nucleus. For the case at hand, all these inequalities are satisfied by a factor of 10^4 or more. A similar analysis, but with $\omega_0 = 0$, has been used in our past work to extract τ_c values near T_C for the cubic ferromagnets Fe and Ni.¹⁰

To describe anisotropic fluctuations we write

$$G_2(t) = S_0 + S_{1a} \exp(-t/\tau_R) \cos(\omega_0 t) + S_{1b} \exp(-4t/\tau_R) \cos(\omega_0 t) + S_2 \exp(-t/\tau_R) \cos(2\omega_0 t) + S_3 \exp(-4t/\tau_R) \cos(3\omega_0 t), \quad (5)$$

with τ_R defined as before, but with the interaction given by $\hbar A I_z S_z$. Equation (5) may be obtained via a generalization of a stochastic model of Blume¹¹ for the case when a static quadrupole interaction is perturbed by a classical uniaxial hyperfine field fluctuating along the principal axis of the electric field gradient. Physically, the Blume model means that only spin fluctuations along the c axis exhibit critical slowing down, whereas spin fluctuations in other directions remain fast with an average of zero. As in the isotropic case the result of Eq. (5) is restricted to the motional narrowing regime.

The principal differences between the isotropic and anisotropic models are the following.

(1) The isotropic model is characterized by a single nuclear relaxation time, τ_R . In contrast, the anisotropic model involves two relaxation times, τ_R and $\tau_R/4$.

(2) The isotropic model has no time-independent "hard core," i.e., $G_2(t) \rightarrow 0$ as $t \rightarrow \infty$. In contrast, the anisotropic model has a hard core, i.e., $G_2(t) \rightarrow 0.2$ as $t \rightarrow \infty$.

In analyzing our data we found that spectra for both crystal orientations were well fitted by the isotropic model for $T > T_C + 1$ K, i.e., reduced temperatures $t > 3 \times 10^{-3}$. In contrast, for $t < 3 \times 10^{-3}$ we observed increasing failure of the isotropic model. As shown in Fig. 4(a), the fitted values of the dominant amplitudes decline whereas the other two amplitudes rise to compensate in part. Given the fixed orientation of the crystal, such amplitude variation is not expected. Close examination of the fitted spectra in the region $t < 3 \times 10^{-3}$ shows substantial misfitting near zero time [Fig. 5(a)]. We conclude that the results are artifacts of fitting with an inapplicable model.

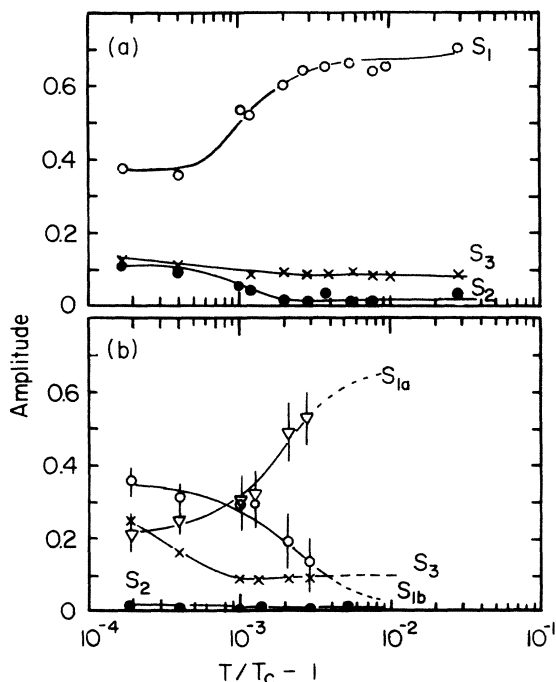


FIG. 4. Amplitude variation for various frequency terms obtained from fitting the PAC data to the isotropic model (a) and the anisotropic model (b). For definitions of the amplitudes, see the text.

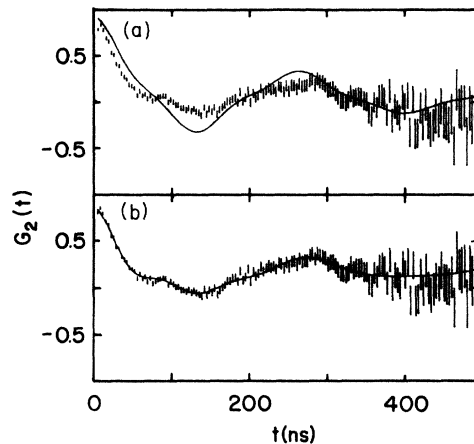


FIG. 5. Comparative quality of fitting obtained via the isotropic model (a) and the anisotropic model (b) for a reduced temperature $t < 10^{-3}$.

We offer two conjectures that might explain the behavior of the PAC spectra in the region $t < 3 \times 10^{-3}$. (1) We may be seeing rounding of the phase transition, so that the PAC signal becomes a superposition of paramagnetic and a ferromagnetic spectra. (2) We may be in a crossover region between isotropic and anisotropic behavior.

Whereas T_C rounding is always present at some level in experiments, the degree of rounding needed to explain our amplitude anomaly is much larger than our measurements in the ferromagnetic region would suggest. As already noted, our T_C value has an error of less than 2×10^{-4} in reduced temperature, and the data below T_C , illustrated in Fig. 3, exhibited no spurious changes in amplitude to within 0.2 K of T_C .

To explore the possibility of a transition to anisotropic behavior, we refitted the data to the anisotropic model. We obtained amplitude variation as shown in Fig. 4(b). The results for $t > 3 \times 10^{-3}$ are equivalent to those of the isotropic model in the sense that a single amplitude for $\cos \omega_0 t$ dominates. (The presence or absence of a relaxation factor multiplying S_0 plays a negligible role in our analysis.) However, fits to the anisotropic model are considerably better for $t < 10^{-3}$, as shown in Fig. 5(b).

We conclude that the failure of the isotropic model close to T_C can be explained by a transition to a regime of anisotropic fluctuations, with spin alignment and fluctuations restricted to the c axis.

III. ANALYSIS OF RELAXATION TIMES

The spin autocorrelation time is defined as the integral of the dynamic structure factor, $S_c(\mathbf{q}, \omega)$, evaluated at zero frequency, over the Brillouin zone of volume v_q :

$$\tau_c = \int_{v_q} S_c(\mathbf{q}, 0) d\mathbf{q} . \quad (6)$$

By recourse to the dynamic scaling theory, $S_c(\mathbf{q}, \omega)$ may be expressed in terms of the power law^{10,12}

$$\tau_c = D t^{-w} , \quad (7)$$

where $t = (T/T_C - 1)$ is the reduced temperature. The ex-

ponent w is given via the scaling law

$$w = \nu(z + 2 - d - \eta), \quad (8)$$

which connects it to other critical exponents ν , z , and η , and the lattice dimensionality, all defined in the usual manner.^{10,12}

Theoretical predictions^{12,13} for three relevant model Hamiltonians are summarized in Table I, using the most accurate available values of ν , z , and η . In earlier work we showed that the behavior of Fe and Ni is consistent with predictions for the Heisenberg model with a nonconserved order parameter.¹⁰ For Gd we expect either similar behavior or Ising behavior.

Experimental values of $\tau_R(T)$, obtained via fitting to the isotropic model, and τ_c values deduced via Eq. (4) are listed in Table II. To extract the exponent w we fixed T_C either at 291.85 K, the value obtained from fitting β , or at nearby values, and fitted to

$$\tau_c(T) = D(T/T_C - 1)^{-w} + \tau_0 \quad (9)$$

with D , W , and τ_0 free. Here τ_0 describes a noncritical background component which we assume to be constant over the range of temperatures studied. Results for these fits are summarized in Table III, top three lines. As is usual in power-law fitting, there is significant covariation of fitting parameters.

To emphasize the region near T_C , where statistics are better and the background is less important, we restricted the reduced temperature to $t < 2 \times 10^{-2}$ and fixed the background to 5.3×10^{-13} s. Under these circumstances we obtained the results summarized in Table III, middle three lines.

Because of the transition to anisotropic behavior, we should expect that data in the transition region analyzed via isotropic assumptions will yield incorrect τ_c values. We have therefore eliminated data for $t < 2 \times 10^{-3}$ and refitted to Eq. (9), with τ_0 and T_C fixed as before. This leads to the results shown in Table III, bottom three lines.

For comparison to theory we use the latter fits to arrive at the final result:

TABLE I. Critical exponent predictions for $d=3$ ferromagnets. Values of β , γ , ν , and η were taken from Ref. 13 and represent the most accurate predictions of renormalization-group theory. Values of α were derived via the scaling law $\alpha + 2\beta + \gamma = 2$. Values of z are based on the predictions $z = \frac{1}{2}(5 - \eta)$, $z = 2 - \eta/2$, and $z = 2 + \alpha/\nu$ for the three columns left to right, as given in Ref. 4. Values of w were derived via the scaling law $w = \nu(z + 2 - d - \eta)$.

Exponent	Heisenberg model		Ising model
	Spin conserved	Spin nonconserved	
β		0.3645(25)	0.3250(20)
γ		1.386(4)	1.2410(20)
ν		0.705(3)	0.6300(15)
η		0.033(4)	0.031(4)
α		-0.115(5)	+ 0.109(5)
z	2.484(2)	1.984(2)	2.173(5)
w	1.023(5)	0.670(5)	0.718(5)

TABLE II. Experimental results.

T^a (K)	t^b (10^{-3})	τ_R (10^{-6} s)	τ_c (10^{-13} s)
Source A			
291.97	0.41	0.26(2)	56.8(50)
292.15	1.03	0.44(2)	33.2(35)
292.20	1.20	0.52(4)	28.1(20)
292.45	2.05	0.57(5)	25.3(19)
292.70	2.91	0.64(5)	22.8(20)
292.94	3.73	0.63(5)	23.2(16)
293.18	4.56	0.90(9)	16.1(18)
293.42	5.4	0.81(8)	17.9(16)
294.17	7.9	0.92(8)	17.7(14)
294.67	9.7	1.06(11)	13.6(14)
300.01	27.9	1.03(17)	14.2(21)
349.98	199.0	2.05(68)	7.0(23)
Source B			
296.0	14.2	1.10(13)	13.0(14)
296.15	14.7	1.11(16)	13.2(20)
298.15	21.6	0.71(11)	20.5(31)
300.15	28.4	1.71(43)	8.6(20)
310.15	62.7	1.78(42)	8.2(19)
320.15	96.9	1.39(31)	10.5(23)
332.65	140.0	1.55(35)	9.4(21)
341.65	171.0	2.31(91)	6.2(15)
354.30	214.0	2.35(72)	6.2(19)
367.03	258.0	1.39(34)	10.3(21)
379.15	299.0	2.67(122)	5.5(25)
395.15	353.0	3.45(260)	4.1(29)
415.0	387.0	2.82(118)	5.1(19)

^aErrors in T average 0.05 K.

^bReduced temperatures based on $T_C = 291.85$ K.

$$w = 0.53(8),$$

$$D = 0.80(35) \times 10^{-13} \text{ s},$$

where

$$2 \times 10^{-3} < t < 2 \times 10^{-2}.$$

A logarithmic plot of background corrected spin autocorrelation times is shown in Fig. 6. This indicates that despite large statistical scatter far from T_C , data for $t < 2 \times 10^{-2}$ are characterized by a well-defined power law. The transition to anisotropic behavior does not appear to be visible at the level of statistical error in our data.

IV. SUMMARY AND CONCLUSION

Our findings may be summarized as follows.

(1) For $t > 3 \times 10^{-3}$, i.e., to within 1 K of T_C , PAC data are well fitted by a model for isotropic spin fluctuations.

(2) For $t < 3 \times 10^{-3}$, i.e., within 1 K of T_C , PAC data undergo a transition which can be explained by a model for anisotropic spin fluctuations along the c axis.

(3) Even in the region in which the isotropic model fits well, the critical exponent w , characterizing the wavevector-averaged spin autocorrelation times, does not cor-

TABLE III. Fitting results for $T > T_c$. [] indicates the parameter is fixed in fitting.

T_c (K)	w	D (10^{-3} s)	τ_0 (10^{-13} s)
$t < 4 \times 10^{-1}$			
[291.80]	0.54(8)	0.72(40)	5.8(14)
[291.85]	0.49(7)	0.98(48)	5.3(16)
[291.90]	0.41(6)	1.54(66)	4.3(16)
$t < 2 \times 10^{-2}$			
[291.80]	0.54(8)	0.74(21)	[5.3]
[291.85]	0.50(4)	0.90(21)	[5.3]
[291.90]	0.45(3)	1.19(21)	[5.3]
$2 \times 10^{-3} < t < 2 \times 10^{-2}$			
[291.80]	0.55(7)	0.75(27)	[5.3]
[201.85]	0.53(7)	0.80(29)	[5.3]
[291.90]	0.51(6)	0.88(31)	[5.3]

respond to predictions for the order-parameter nonconserving Heisenberg model (Table I), but has a lower value. It also does not agree with predictions for the Ising model.

Our results may be compared to Mössbauer work^{5,7} on $Gd^{161}Dy$, in which we found $w=0.49(5)$ in the range $10^{-3} < t < 10^{-1}$. In that work, being unable to distinguish isotropic from anisotropic behavior, we assumed isotropic spin fluctuations in order to analyze the critical component of the Mössbauer linewidth. Since the Mössbauer study and the present work cover roughly the same range in reduced temperature, it is perhaps not surprising that the values of w agree for the two studies. As in the present work, the Mössbauer work shows no significant deviation in the power law in the neighborhood of $t=3 \times 10^{-3}$ where the PAC data suggest the onset of anisotropic spin fluctuations.

How do we explain the anomalous value of w in two in-

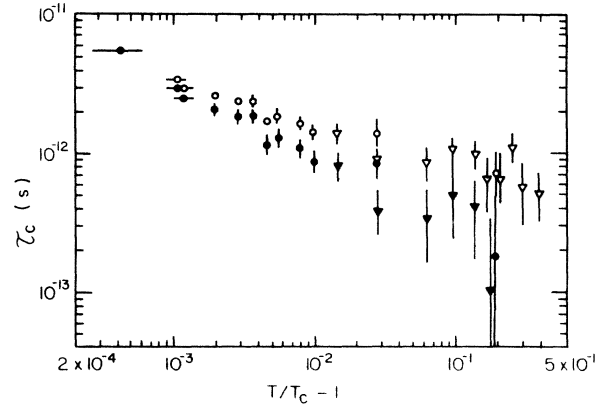


FIG. 6. Logarithmic plot of the spin autocorrelation time versus the reduced temperature with and without correction for noncritical background (solid) and open symbols, respectively. Data are shown for sources *A* (circles) and *B* (triangles).

dependent experiments? The most likely cause is that we are measuring in a broad crossover region in which we cannot reach either asymptotic Heisenberg or Ising behavior because Ising-like anisotropic spin fluctuations separate the experimentally accessible region from the critical point. If this is the case one can also understand why past measurements of static critical exponents in Gd , which are all confined to $t > 10^{-3}$, do not yield clear-cut Heisenberg or Ising values, but include a mix of both.^{5,8}

ACKNOWLEDGMENTS

Help in data analysis was received from Nicholas Rosov and Reinhardt Schuhmann. Useful critical comments were made by Alfred Kleinhammes. The National Science Foundation provided research support under Grant No. DMR-83-03611.

*Present address: Department of Physics, Washington State University, Pullman, WA 99164.

† Present address: Department of Physics, University of Central Florida, Orlando, FL 32816.

¹J. W. Cable and E. O. Wollan, *Phys. Rev.* **165**, 733 (1965).

²F. Milstein and L. B. Robinson, *Phys. Rev.* **177**, 904 (1969).

³G. Boström, B. Liljgren, B. Jonsson, and E. Karlson, *Phys. Scr.* **3**, 175 (1971).

⁴P. Molho and J. L. Porteseil, *J. Phys. (Paris)* **44**, 83 (1983).

⁵A. R. Chowdhury, G. S. Collins, and C. Hohenemser, *Phys. Rev. B* **30**, 6277 (1984).

⁶A. R. Chowdhury, G. S. Collins, and C. Hohenemser, *Phys. Rev. B* (to be published).

⁷A. R. Chowdhury, G. S. Collins, and C. Hohenemser, *Phys.*

Rev. B (to be published).

⁸A. R. Arends, C. Hohenemser, F. Pleiter, H. de Waard, L. Chow, and R. M. Suter, *Hyperfine Interact.* **8**, 191 (1980).

⁹A. Abragam and R. V. Pound, *Phys. Rev.* **92**, 943 (1953).

¹⁰C. Hohenemser, L. Chow, and R. M. Suter, *Phys. Rev. B* **26**, 5056 (1982).

¹¹M. Blume, in *Hyperfine Structure and Nuclear Radiation*, edited by E. Matthias and D. A. Shirley (Amsterdam, North Holland, 1968), p. 911.

¹²P. C. Hohenberg and B. I. Halperin, *Rev. Mod. Phys.* **49**, 435 (1977).

¹³J. C. Le Guillou and J. Zinn-Justin, *Phys. Rev. Lett.* **39**, 95 (1977).